DOI: 10.1002/ange.201101210

Inhibitor Design

Structure-Guided Development of Selective RabGGTase Inhibitors**

*Robin S. Bon, Zhong Guo, E. Anouk Stigter, Stefan Wetzel, Sascha Menninger, Alexander Wolf, Axel Choidas, Kirill Alexandrov, Wulf Blankenfeldt, Roger S. Goody, and Herbert Waldmann**

Rab guanosine triphosphatases (GTPases) are key players in the regulation of eukaryotic intracellular trafficking events such as the formation, motility, targeting, and docking of vesicles.[1] The reversible association of Rab GTPases with intracellular membranes and other proteins is essential for their function, and is mediated by geranylgeranyl (GG) group(s) covalently attached to C-terminal cysteine residues. This modification, known as prenylation, is mediated by the enzyme Rab geranylgeranyl transferase (RabGGTase) in concert with the accessory Rab escort protein (REP).[2]

[*] Dr. R. S. Bon,[+] E. A. Stigter,[+] Dr. S. Wetzel, Prof. Dr. H. Waldmann
Max-Planck-Institut für molekulare Physiologie
Abt. Chemische Biologie
Otto-Hahn-Strasse 11, 44227 Dortmund (Germany)
and
TU Dortmund, Fakultät Chemie, 44227 Dortmund (Germany)
Fax: (+49) 231-133-2499
E-mail: herbert.waldmann@mpi-dortmund.mpg.de
Dr. Z. Guo,[+] Prof. Dr. K. Alexandrov, Dr. W. Blankenfeldt, Prof. Dr. R. S. Goody
Max-Planck-Institut für molekulare Physiologie
Abt. Physikalische Biochemie
Otto-Hahn-Strasse 11, 44227 Dortmund (Germany)
Dr. S. Menninger, Dr. A. Wolf, Dr. A. Choidas
Lead Discovery Center GmbH
Emil-Figge-Strasse 76a, 44227 Dortmund (Germany)
Dr. R. S. Bon[+]
Current address: School of Chemistry and Biomedical and Health Research Centre, University of Leeds, Leeds, LS2 9JT (UK)
Dr. S. Wetzel
Current address: Quantitative Biology, Developmental and Molecular Pathways, Novartis Institutes of Biomedical Research Basel (Switzerland)
Dr. Z. Guo,[+] Prof. Dr. K. Alexandrov
Current address: Institute for Molecular Bioscience
The University of Queensland, Brisbane, Queensland (Australia)
Dr. W. Blankenfeldt
Current address: University of Bayreuth, Bayreuth (Germany)
[+] These authors contributed equally.

[**] We thank the X-ray communities of the Max-Planck-Institut für molekulare Physiologie (Dortmund, Germany) and the Max-Planck-Institut für medizinische Forschung (Heidelberg, Germany) for collecting diffraction data at the Swiss Light Source of the Paul Scherrer Institute (Villigen, Switzerland) and for giving us generous access to and support with station X10SA. This work was supported in part by DFG grants to H.W. and R.S.G. (grant no.: SFB642), and by the Zentrum für Angewandte Chemische Genomik. R.S.B. thanks the Alexander von Humboldt Stiftung for a fellowship. E.A.S thanks the IMPRS-CB for a PhD scholarship.

Supporting information for this article is available on the WWW under http://dx.doi.org/10.1002/anie.201101210.

The overexpression of RabGGTase and its substrates such as Rab5a, Rab7, and Rab25 in several cancer types[3] and the finding that RabGGTase inhibition leads to p53-independent apoptosis[4] validate RabGGTase as a promising anticancer target. Whereas numerous inhibitors of the related CaaX prenyl transferases, farnesyl transferase (FTase),[5] and geranylgeranyl transferase I (GGTase I)[6] have been developed and have even reached clinical trials,[7] in most cases their cellular targets are not known with certainty. Very few RabGGTase inhibitors are known to date,[8] many of which are either nonselective with respect to FTase or show only moderate inhibition of cellular Rab prenylation.

The most potent of the currently available RabGGTase inhibitors, BMS3, was originally designed as an FTase inhibitor.[4] Since BMS3 lacks selectivity with respect to FTase, both in vitro[4] and in cells,[9] its pro-apoptotic effect could only be attributed to RabGGTase inhibition indirectly. Selective inhibitors of RabGGTase would be valuable for analysis of the effects of selective inhibition of Rab trafficking on the proliferation of transformed cells, for the elucidation of side effects related to FTase inhibition, and, in general, for the analysis of Rab-mediated cellular processes. With these goals in mind, we chose to generate cocrystal structures of RabGGTase and FTase with BMS3 and use this structural information to design RabGGTase-specific inhibitors.

Herein we report the structure-guided design of selective RabGGTase inhibitors with potent cellular activities. The inhibitors target the RabGGTase-specific tunnel adjacent to the GGPP binding site (TAG tunnel), which was recently found in a cocrystal structure of an RabGGTase-peptide-based inhibitor.[8b] Since this TAG tunnel is a unique feature that distinguishes RabGGTase from FTase and GGTase I, it provides a rational molecular basis to achieve selectivity.

To enable rational design of the inhibitor, we synthesized BMS3, soaked it into both RabGGTase and FTase, and solved the binary RabGGTase:BMS3, the ternary RabGGTase:BMS3:GGPP, and the ternary FTase:BMS3:FPP cocrystal structures (Figure 1).

The binding modes and conformations of BMS3 in these structures are highly similar. In both enzymes the imidazole ring coordinates to the catalytic zinc ion, whilst the phenyl ring of the tetrahydrobenzodiazepine (THB) core π stacks with the Tyr361 or the Phe289 residue. The 3-benzyl moiety extends toward the lipid binding sites in both enzymes and is involved in extensive T stacking with hydrophobic residues of the enzymes (Figure 1). These common interaction patterns result in the twisted form of the central 3-benzyl-THB unit that is observed in both enzymes. The anisylsulfonyl substituent adopts a pseudoaxial position and is involved in internal π-stacking interactions. In RabGGTase, an additional

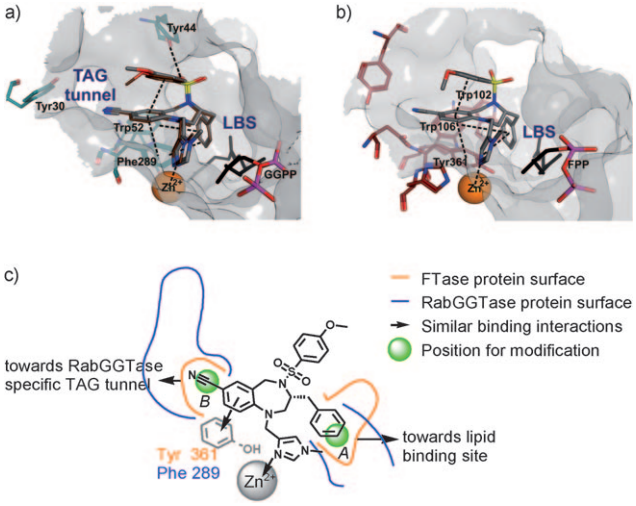

Figure 1. Cocrystal structures of BMS3: a) Surface representation of the active site of the BMS3:RabGGTase:GGPP complex (PDB access code: 3PZ2). The imidazole ring coordinates to the zinc ion, whereas the sulfonamide forms hydrogen bonds with Tyr44. The 3-benzyl moiety interacts with Trp52 and Phe289 by T stacking, whereas the tetrahydrobenzodiazepine (THB) moiety π stacks with Phe289. The conformation is further stabilized by internal π stacking of the THB with the anisolylsulfonyl group. The nitrile points toward the TAG tunnel. The orientation of BMS3 in the binary complex BMS3:RabGGTase is depicted in brown lines (PDB access code: 3PZ1). The black dashed lines indicate interactions between the ligand and the enzyme. b) Surface representation of the active site of the BMS3:FTase:FPP complex (PDB access code: 3PZ4); the imidazole ring coordinates to the zinc ion. The 3-benzyl moiety interacts with Trp102 and Trp106 by T stacking. The THB moiety interacts with Tyr361 and is further involved in internal π stacking with the anisylsulfonyl group, which is mainly exposed to solvent. The black dashed lines indicate interactions between the ligand and the enzyme. c) Schematic representation of the common binding modes of BMS3 in Figure 1a and b.

hydrogen-bond interaction is formed between the sulfonyl group and Tyr44, whereas this group is mostly solvent exposed in FTase. In RabGGTase:BMS3:GGPP, the nitrile group of BMS3 is close to the TAG tunnel, whereas this group is close to the protein surface in FTase:BMS3:FPP, where it is merely involved in dipolar interactions with hydrophobic residues. The shared binding interactions are reflected in similar inhibition data for FTase and RabGGTase, as reported in the literature (in vitro radiometric assay: $IC_{50} = 1.4$ nM and 16 nM, respectively[4] and inhibition of cellular prenylation: $K_i = 7$ nM and 50 nM, respectively[9]). These data confirm that BMS3 is a highly potent dual inhibitor of FTase and RabGGTase.

To obtain selective RabGGTase inhibitors, we considered several structure-guided modifications of BMS3. We decided to keep the anisylsulfonyl and imidazole substituents of BMS3 in our analogues. The imidazole was kept because it represents the crucial zinc binding group. The anisylsulfonyl moiety was already shown to be highly variable in FTase without leading to significant changes in activity,[10] whereas this group is involved in hydrogen bonding to Tyr44 in RabGGTase. Therefore, we expected to observe no significant gain in selectivity for RabGGTase by varying this group, and decided to retain it to ensure the positive internal π-stacking interaction.

Since the TAG tunnel is a unique feature of RabGGTase, the introduction of moieties larger than the nitrile at position *B* were expected to fit well in to the RabGGTase TAG tunnel but would clash with the FTase surface. Furthermore, we envisioned that hydrogen-bond acceptors would interact with the nearby Tyr30 (see also Figure S2b in the Supporting Information).

The 3-benzyl group of BMS3 approaches the lipid binding sites (LBSs) of both enzymes. In FTase, the bulky Trp102, which ensures the selectivity for FPP over GGPP, is close to the 3-benzyl moiety and is involved in T-stacking interactions. In RabGGTase, this tryptophan residue is replaced by a small serine residue and, therefore, forms a larger binding cavity (see Figure S2a in the Supporting Information). We predicted that the introduction of larger groups at position *A* (Figure 1c) would result in selectivity for RabGGTase over FTase as a result of an expected steric clash with Trp102.

Thus, we envisioned that extension of BMS3 at positions *A* and *B* (Figure 1c) would lead to selective inhibitors of RabGGTase. A virtual high-throughput screening (VHS) was conducted to identify promising substituents.[11] The virtual library was enumerated by decorating the core scaffold with different substituents at positions *A* and *B*, and was screened with both enzymes (for details, see the Supporting Information). The docking scores were compared, and compounds that gave good results for RabGGTase and poor results for FTase were selected. These promising candidates were evaluated further, prioritized by individual docking, and selected for synthesis.

Two general building blocks, **3a** and **3b**, were synthesized according to modified literature procedures.[10] A condensation of 5-bromoisatoic anhydride (**1**) and D-tyrosine methyl ester resulted in the benzodiazepine core, with the phenolic hydroxy group and the bromo substituents introduced as versatile synthetic handles for modification (Scheme 1). Subsequent reduction with borane afforded **2a**, and a subsequent copper-catalyzed cyanation resulted in **2b**. Selective *N*-sulfonylation with 4-methoxybenzenesulfonyl chloride in pyridine and reductive amination with 4-imidazocarbox-

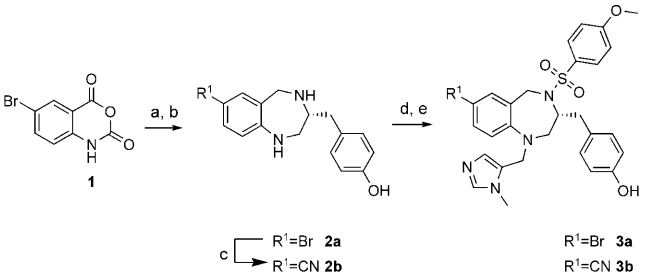

Scheme 1. Synthesis of general building blocks. a) D-Tyr-OMe·HCl, DMAP, pyridine, 3 days, reflux; b) BH_3 in THF, 16 h, reflux (62%, 2 steps); c) CuCN, DMF, 0.5 h, microwaves 210°C (67%); d) 4-methoxybenzenesulfonylchloride, pyridine, 16 h, RT (61–71%); e) *N*-methylimidazole-5-carboxaldehyde, TFA, TFAA, Et_3SiH, CH_2Cl_2, 16 h, RT (80–83%). DMAP = 4-dimethylaminopyridine, TFA = trifluoroacetic acid.

aldehyde in the presence of trifluoroacetic anhydride (TFAA) as a water scavenger[12] resulted in building blocks **3a** and **3b** in 38 and 26% overall yield, respectively. Substituents meant to target the hydrophobic binding pocket (R^2) were attached by alkylation or aminocarbonylation, (Scheme 2, compounds **4**–**7**). Groups meant to target the TAG tunnel (R^1) were introduced by substitution of the aryl bromide under Suzuki coupling conditions (Scheme 2, compounds **8**–**12**) in 30–80% overall yield and high purity.

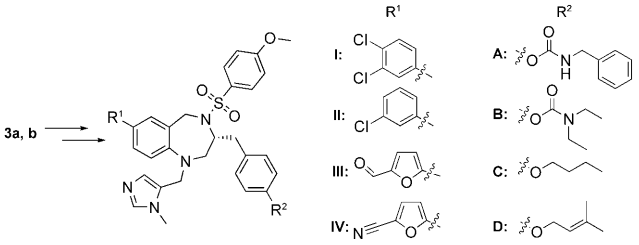

Scheme 2. Modification of **3a**,**b**.

The collection was screened using fluorometric FTase[13] and RabGGTase assays.[14] These fluorometric assays are continuous and less-laborious alternatives to the corresponding radioactivity-based assays. For BMS3, we determined an IC_{50} value of 724 nM for RabGGTase and an IC_{50} value of 6 nM for FTase (Table 1). The pronounced difference in IC_{50} values for these enzymes compared to previously reported values from radiometric assays[4] is related to the use of artificial fluorescent substrates in these assays. Therefore, we introduced the improvement factor (IF) to indicate the improvement in selectivity for RabGGTase, compared to the dual inhibitor BMS3 (see above). In addition IC_{50} values for GGTase I were measured to evaluate the selectivity of our THB-based inhibitors with respect to all three prenyl transferases.

As expected on the basis of VHS, modification at R^2 led to a general increase in selectivity for RabGGTase. The expected clash with Trp102 in the LBS of FTase resulted in a one–threefold decrease in FTase inhibition, but did not lead to a loss of activity. Therefore, it is likely that the inhibitors and/or FTase adapt their binding conformation to the newly introduced moieties.

Modification at R^1 showed a sharper inhibition profile. Whereas **9** and **10** showed moderate to good RabGGTase inhibitory activity, **8** showed very poor inhibition. The 4-chlorophenyl substituent could result in a clash with the RabGGTase surface, if it is assumed that the THB–core binding mode is very rigid (Figure 2a). This clash was successfully circumvented by the introduction of a slightly smaller five-membered ring, which indeed resulted in an increase in selectivity. Although an increase in selectivity was reached by modifying one side of BMS3 (**4**–**7**, **9**–**11**), and variation of R^2 contributed more to a gain in selectivity than did variation of R^1, the single modifications we explored did not result in full selectivity. However, the combination of modification III or IV and A resulted in fully selective RabGGTase inhibitors **14** and **15**.

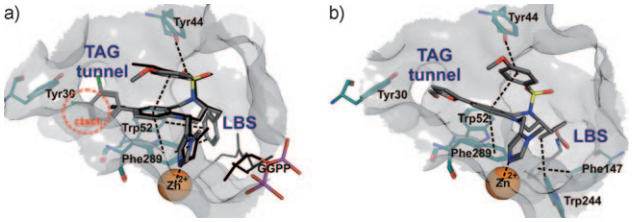

Figure 2. a) Individual docking results of **8** as well as an overlay with the structure of BMS3:RabGGTase:GGPP. Assuming a rigid THB–core binding arrangement, the *para*-chlorophenyl group cannot adjust its position toward the TAG tunnel, and clashes with the binding pocket. b) Cocrystal structure of **14**:RabGGTase (PDB access code: 3PZ3); the furanaldehyde substituent is located in the entrance of the TAG tunnel, but does not show the expected hydrogen-bond interaction with Tyr30. The benzylcarbamate group is situated in the LBS and T stacks with Phe147. The 3-benzyl moiety is reoriented and T stacks with Trp244. The black dashed lines indicate interactions between the ligand and the enzyme.

Table 1: In vitro activity of the THB library.

Cmpd	R^1	R^2	RabGGTase IC_{50} [nM]	FTase IC_{50} [nM]	GGTase I IC_{50} [nM]	IF[a]
BMS3	CN	H	724±321	6±3	>99500	1
4	CN	**A**	72±2	<5[b]	>99500	<8
5	CN	**B**	38±7	<5[b]	2020±384	<16
6	CN	**C**	162±10	10±7	>99500	7
7	CN	**D**	39±10	15±8	>99500	46
8	**I**	OH	>9500	194±78	>99500	<2
9	**II**	OH	1302±478	42±10	>99500	4
10	**III**	OH	206±13	7±3	>99500	4
11	**IV**	OH	63±2	13±3	>99500	25
12	**II**	**A**	2264±844	123±24	>99500	7
13	**II**	**C**	6515±1839	>9700	>99500	>180
14	**III**	**A**	141±26	>9700	>99500	>8301
15	**IV**	**A**	42±13	>9700	>99500	>27868

[a] The improvement factor (IF) shows the relative increase in selectivity for RabGGTase versus FTase compared to the original compound BMS3, for which this value is 1 by definition. [b] Lower detection limit.

The RabGGTase:**14** cocrystal structure shows that **14** binds in a mode similar to BMS3, with the imidazole ring coordinating to the catalytic zinc ion and the THB core of **14**, although it is slightly twisted compared to BMS3. It also π stacks with Phe289. In agreement with the predictions from docking studies, the benzyl carbamate occupies the lipophilic substrate binding site of RabGGTase, while the furanal substituent approaches the TAG tunnel. The arrangement of the benzylcarbamate in the LBS results in an extra T stacking to Phe147, as well as a conformational change of the 3-benzyl substituent, which now T stacks with Trp244 instead of with Phe289 and Trp52. Surprisingly, the aldehyde moiety is not involved in a hydrogen-bonding interaction with Tyr30, but points into the TAG tunnel.

To determine whether the compounds inhibit Rab prenylation in cellular systems, cultured HeLa cells were incubated with the inhibitors for 6 h and then lysed. The lysate was subjected to in vitro reprenylation with recombinant RabGG-

Tase, REP, and biotin-GPP (a GGPP analogue), and then the Rab-biotin-GPP conjugates were detected by Western blotting (see the Supporting Information).[9] Compounds **4**–**7**, **9**–**11**, **14**, and **15** all caused increased labeling of endogenous Rab proteins with biotin-GPP, thus indicating inhibition of cellular prenylation, with IC_{50} values in the nanomolar range (Table 2).[15] Furthermore, the cellular IC_{50} values roughly follow the in vitro data, thus indicating that the modifications did not significantly affect the bioavailability. As expected, compound **8**, which was inactive in vitro, did not inhibit cellular Rab prenylation.

Table 2: Reprenylation assay results of THB library compounds.

Cmpd	Reprenylation rel. IC_{50} [nM][a]	Cmpd	Reprenylation rel. IC_{50} [nM][a]
BMS3	74 ± 34	**9**	201 ± 78
4	81 ± 32	**10**	93 ± 42
5	343 ± 29	**11**	11 ± 5
6	307 ± 40	**14**	311 ± 193
7	43 ± 12	**15**	49 ± 32
8	> 30000		

[a] For the calculation of relative IC_{50} values, the signal obtained from the positive control (1 μM BMS3, which gives a saturated reprenylation signal) was set as 100% RabGGTase inhibition.

Next, we studied the effect of several inhibitors on the viability of mammalian cancer cell lines and peripheral blood mononuclear cells (PBMC; Table 3). In these experiments, cultured cells were incubated with a THB for 72 h, followed by incubation with resazurin. Viable cells reduce resazurin to the fluorescent resorufin. Therefore, fluorescence intensity is a measure of cell viability.[15]

Table 3: Cellular viability assay data (IC_{50}, [nM]).[a]

Cmpd	HCT116	A2780	HeLa	PBMC
BMS3	63 ± 8	43 ± 0	101 ± 2	> 10000
4	230 ± 59	130 ± 9	151 ± 21	> 10000
5	75 ± 10	43 ± 9	745 ± 303	> 10000
7	112 ± 2	111 ± 1	59 ± 2	> 10000
11	2 ± 1	18 ± 1	21 ± 4	> 10000
14	443 ± 173	589 ± 199	797 ± 330	> 10000
15	35 ± 1	115 ± 3	101 ± 11	> 10000

[a] The IC_{50} values for individual compounds reflect the inhibition of cell proliferation. The compounds were evaluated against a DMSO control. For further details, see the Supporting Information.

As can been seen in Table 3, the tested THBs were not generally toxic to blood cells, but proved to be potent inhibitors of the proliferation of three cancer cell lines. The IC_{50} values in this assay generally follow the trends of the cellular Rab prenylation assay. Most importantly, highly selective RabGGTase inhibitor **15** inhibits cancer cell proliferation as potently as the dual RabGGTase/FTase inhibitor BMS3, whereas the somewhat lower potency of THB **14** corresponds well with its decreased potency as a cellular Rab prenylation inhibitor. The most potent inhibitor of cellular Rab prenylation, THB **11**, which is also a highly potent FTase inhibitor, is also the most potent inhibitor of cancer cell proliferation. The inhibition of cancer cell proliferation (both Ras-transformed and non-Ras-transformed) by the highly selective RabGGTase inhibitors **14** and **15** is in accordance with the finding that RabGGTase siRNA, but not FTase siRNA, induces increased apoptosis in *C. elegans* and A549 cells.[4] Therefore, these results emphasize that RabGGTase should be considered an anticancer target.

In conclusion, by applying protein/inhibitor cocrystal structure analysis, VHS, individual docking, and synthesis we have identified potent and selective RabGGTase inhibitors that inhibit proliferation of several cancer cell lines without displaying cytotoxicity in PBMC cells. Guided by the well-defined binding mode and conformation of BMS3 in RabGGTase and FTase in the cocrystal structures, we have shown that it is possible to make BMS3 analogues that are selective for RabGGTase. This has been achieved by exploiting recently identified structural features of the RabGGTase active site such as a combination of the TAG tunnel and lipid binding site. These results also indicate that RabGGTase-THB cocrystal structures might be a valuable starting point for more extensive structure-based design of selective RabGGTase inhibitors, for example by using computational methods based on fragment docking and growing/linking approaches.

Received: February 17, 2011
Published online: April 21, 2011

Keywords: antitumor agents · drug design · inhibitors · protein modification · transferases

[1] M. Zerial, H. McBride, *Nat. Rev. Mol. Cell Biol.* **2001**, *2*, 107–117.
[2] a) K. F. Leung, R. Baron, M. C. Seabra, *J. Lipid Res.* **2006**, *47*, 467–475; b) K. T. Lane, L. S. Beese, *J. Lipid Res.* **2006**, *47*, 681–699.
[3] a) K. W. Cheng, J. P. Lahad, W. L. Kuo, A. Lapuk, K. Yamada, N. Auersperg, J. S. Liu, K. Smith-McCune, K. H. Lu, D. Fishman, J. W. Gray, G. B. Mills, *Nat. Med.* **2004**, *10*, 1251–1256; b) K. Croizet-Berger, C. Daumerie, M. Couvreur, P. J. Courtoy, M. F. van den Hove, *Proc. Natl. Acad. Sci. USA* **2002**, *99*, 8277–8282.
[4] M. R. Lackner, R. M. Kindt, P. M. Carroll, K. Brown, M. R. Cancilla, C. Y. Chen, H. de Silva, Y. Franke, B. Guan, T. Heuer, T. Hung, K. Keegan, J. M. Lee, V. Manne, C. O'Brien, D. Parry, J. J. Perez-Villar, R. K. Reddy, H. J. Xiao, H. J. Zhan, M. Cockett, G. Plowman, K. Fitzgerald, M. Costa, P. Ross-Macdonald, *Cancer Cell* **2005**, *7*, 325–336.
[5] a) S. M. Sebti, A. D. Hamilton, *Oncogene* **2000**, *19*, 6584–6593; b) R. A. Gibbs, T. J. Zahn, J. S. Sebolt-Leopold, *Curr. Med. Chem.* **2001**, *8*, 1437–1465.
[6] F. El Oualid, L. H. Cohen, G. A. van der Marel, M. Overhand, *Curr. Med. Chem.* **2006**, *13*, 2385–2427.
[7] a) A. D. Basso, P. Kirschmeier, W. R. Bishop, *J. Lipid Res.* **2006**, *47*, 15–31; b) P. A. Konstantinopoulos, M. V. Karamouzis, A. G. Papavassiliou, *Nat. Rev. Drug Discovery* **2007**, *6*, 541–555; c) A. Kazi, A. Carie, M. A. Blaskovich, C. Bucher, V. Thai, S. Moulder, H. Peng, D. Carrico, E. Pusateri, W. J. Pledger, N. Berndt, A. Hamilton, S. M. Sebti, *Mol. Cell. Biol.* **2009**, *29*, 2254–2263.
[8] a) M. Watanabe, H. D. G. Fiji, L. Guo, L. Chan, S. S. Kinderman, D. J. Slamon, O. Kwon, F. Tamanoi, *J. Biol. Chem.* **2008**, *283*,

9571 – 9579; b) K. T. Tan, E. Guiu-Rozas, R. S. Bon, Z. Guo, C. Delon, S. Wetzel, S. Arndt, K. Alexandrov, H. Waldmann, R. S. Goody, Y. W. Wu, W. Blankenfeldt, *J. Med. Chem.* **2009**, *52*, 8025 – 8037; c) R. A. Baron, R. Tavare, A. C. Figueiredo, K. M. Blazewska, B. A. Kashemirov, C. E. McKenna, F. H. Ebetino, A. Taylor, M. J. Rogers, F. P. Coxon, M. C. Seabra, *J. Biol. Chem.* **2009**, *284*, 6861 – 6868; d) F. P. Coxon, M. H. Helfrich, B. Larijani, M. Muzylak, J. E. Dunford, D. Marshall, A. D. McKinnon, S. A. Nesbitt, M. A. Horton, M. C. Seabra, F. H. Ebetino, M. J. Rogers, *J. Biol. Chem.* **2001**, *276*, 48213 – 48222; e) C. E. McKenna, B. A. Kashemirov, K. M. Blazewska, I. Mallard-Favier, C. A. Stewart, J. Rojas, M. W. Lundy, F. H. Ebetino, R. A. Baron, J. E. Dunford, M. L. Kirsten, M. C. Seabra, J. L. Bala, M. S. Marma, M. J. Rogers, F. P. Coxon, *J. Med. Chem.* **2010**, *53*, 3454 – 3464; f) Z. Guo, Y. W. Wu, K. T. Tan, R. S. Bon, E. Guiu-Rozas, C. Delon, T. U. Nguyen, S. Wetzel, S. Arndt, R. S. Goody, W. Blankenfeldt, K. Alexandrov, H. Waldmann, *Angew. Chem.* **2008**, *120*, 3807 – 3810; *Angew. Chem. Int. Ed.* **2008**, *47*, 3747 – 3750.

[9] U. T. T. Nguyen, Z. Guo, C. Delon, Y. W. Wu, C. Deraeve, B. Fraenzel, R. S. Bon, W. Blankenfeldt, R. S. Goody, H. Waldmann, D. Wolters, K. Alexandrov, *Nat. Chem. Biol.* **2009**, *5*, 227 – 235.

[10] J. T. Hunt, C. Z. Ding, R. Batorsky, M. Bednarz, R. Bhide, Y. Cho, S. Chong, S. Chao, J. Gullo-Brown, P. Guo, S. H. Kim, F. Y. F. Lee, K. Leftheris, A. Miller, T. Mitt, M. Patel, B. A. Penhallow, C. Ricca, W. C. Rose, R. Schmidt, W. A. Slusarchyk, G. Vite, V. Manne, *J. Med. Chem.* **2000**, *43*, 3587 – 3595.

[11] VHS was carried out using protonated enzyme structures (prepared in Moe) and screened with GOLD. Details can be found in the Supporting Information.

[12] B. C. Chen, J. E. Sundeen, P. Guo, M. S. Bednarz, R. Zhao, *Tetrahedron Lett.* **2001**, *42*, 1245 – 1246.

[13] a) D. L. Pompliano, R. P. Gomez, N. J. Anthony, *J. Am. Chem. Soc.* **1992**, *114*, 7945 – 7946; b) D. L. Pompliano, E. Rands, M. D. Schaber, S. D. Mosser, N. J. Anthony, J. B. Gibbs, *Biochemistry* **1992**, *31*, 3800 – 3807.

[14] a) Y. W. Wu, H. Waldmann, R. Reents, F. H. Ebetino, R. S. Goody, K. Alexandrova, *ChemBioChem* **2006**, *7*, 1859 – 1861; b) Y. W. Wu, K. Alexandrov, L. Brunsveld, *Nat. Protoc.* **2007**, *2*, 2704 – 2711.

[15] For details see the Supporting Information.

